POSITION ANALYSIS AND CONTROL OF A NEW QUADROTOR MANIPULATION SYSTEM

Ahmed Khalifa[*] and Mohamed Fanni[**]

Abstract

In this article, the position kinematic analysis of a novel quadrotor manipulation system is presented. In this system, a quadrotor is attached with 2-DOF robotic arm. The proposed robot addresses the limitations found in the current aerial manipulators. To check the reliability of the proposed system, a quadrotor with high allowable payload capability is selected and the robot arm is designed. Forward and inverse kinematics are derived to be utilized in the control system in order to reach the desired position and orientation of the end-effector. The controller design of the proposed robot is proposed, in the quadrotor/joint space, based on Disturbance Observer (DOb) and compared to an adaptive intelligent controller. Stability analysis of the proposed control system is presented. The two controllers are tested to achieve point-to-point control of the end-effector under the effects of picking/releasing an object, changing the point of operation, and measurement noise. Simulation study is carried out in MATLAB environment. The results show the feasibility of the proposed system, in addition to, the effectiveness of the kinematic analysis and the proposed controller.

Keywords

Aerial Manipulation, Quadrotor, Inverse Kinematics, Disturbance Observer, Stability Analysis

1. Introduction

Recently, Unmanned Aerial Vehicles (UAVs) attracts the research due to their ability of speed and access to regions that are not reached by ground robots. One of them are the Quadrotor that have certain characteristics, such as small size and cost, Vertical Take Off and Landing (VTOL), slow precise movements, which enlighten their capabilities for use in vital applications such as homeland security and earth sciences [1]. However, most research on UAVs has typically been limited to monitoring and surveillance applications where heir tasks are limited to look and search. Due to their superior characteristics, quadrotrs has high interest to be used in aerial manipulation.

[*,**] Department of Mechatronics and Robotics Engineering, Egypt-Japan University of Science and Technology, Egypt; email: ahmed.khalifa@ejust.edu.eg
[**]On leave from Department of Production Engineering and Mechanical Design, Mansoura University, Egypt; email: mohamed.fanni@ejust.edu.eg

Previous research on aerial manipulation can be divided into three approaches. In the first approach, a gripper is mounted at the bottom of an UAV to hold a payload [2], which is utilized in transportation of objects and structure building. However, in this system, the payloads are attached to the body of an UAV rigidly. As a result, the attitude of the object has the same the orientation of the quadrotor, in addition to, the limited range of the end-effector is due to the quadrotor's body.

Secondly, a payload is suspended with cables [3]. In [4], specific attitude and position of a payload is achieved using cables connected to three quadrotors. However, using cables cannot always provide the required motion for the payload.

The third approach concentrates on the interaction with an existing structure, as example, for contact inspection. In [5] research has been conducted on utilizing a force sensor or a brush as a manipulator. However, this approach can be used only in specific tasks such as wall inspection.

To cope up with these limitations, an approach is developed in which the quadrotor is equiped with a robot arm. In [6], a helicopter platform is equipped with dual robotic arm to do aerial manipulation. In [7], a test bed with four-DOF robot arms and a crane emulating an aerial robot is presented. In [8–10] a manipulator with more than two links were used. In [11], a quadrotor with dual robotic arm are combined. However, with these systems, the final payload of the quadrotor is decreased due to the excessive manipulator weight.

In [12], we proposed a new aerial manipulation system that has a two DOF manipulator mounted at the center bottom of a quadrotor. This robot addresses the issues appeared in the currently developed aerial manipulators. Firstly, our proposed robot can manipulate the objects with arbitrary pose. Secondly, it uses a minimum manipulator weight (2-DOF manipulator). Thirdly, using the robot arm allows a significant and controlled distance between the platform and the object. In [13], an aerial manipulator using a quadrotor with a 2-link manipulator is proposed but with different topology such that It can not solve the issue of the limited DOFs of the system. Moreover, the inverse kinematics problem has not been solved yet. The proposed flying robot enlighten new robotic applications such as inspection, firefighting, rescue operation, surveillance, demining, carrying out missions in risky places, and transportation in remote places.

In this article, the design and modeling of the proposed aerial manipulator are described. In addition, the forward/inverse position kinematics analysis are derived which will be utilized to control the end-effector position and orientation. Moreover, a quadrotor/joint space controller is designed based on Disturbance Observer (DOb) technique.
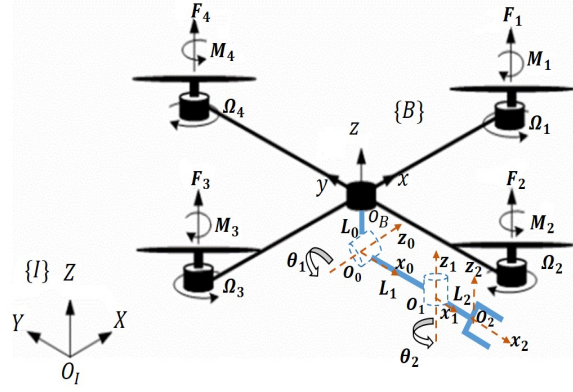
Figure 1: 3D-CAD model of the proposed ystem

Figure 2: Schematic diagram of the system with frames

2. Description and Kinematic Analysis of the Proposed System

Fig. 1 shows the structure of the proposed system. The proposed system consists mainly a quadrotor and a 2-link robotic arm.

A lightweight robot arm that can carry a payload of $200g$ and has maximum reach of $25cm$ is designed. The total weight of the manipulator, including actuators and gripper, is $200g$. The quadrotor components are chosen such that it can carry payload equals $500g$ (larger than the total manipulator weight and the maximum payload).

Fig. 2 presents a sketch of the proposed Quadrotor Manipulation System with the relevant frames. The frames satisfy the Denavit-Hartenberg (DH) convention [14]. The arm has two joints that are revolute. The axis of the 1st one (z_0) is parallel to the quadrotor x-axis (see Fig. 2). The axis of the other one (z_1) will be parallel to the quadrotor y-axis at the extended position. Hence, the pitch and roll rotation of the end-effector can be achieved without moving the quadrotor horizontally. Consequently, with this topology, the arm can manipulate objects in arbitrary pose.

This robot system is described by its position and orientation with respect to an earth-fixed reference frame {I}, O_I-$X\,Y\,Z$. The rotation matrix expressing the transformation from the earth-fixed frame {I} to the body-fixed frame{B}, O_B-x y z, can be defined as:

$$R_I^B = \begin{bmatrix} C(\psi)C(\theta) & S(\psi)C(\theta) & -S(\theta) \\ -S(\psi)C(\phi) + S(\psi)S(\theta)C(\psi) & C(\psi)C(\phi) + S(\psi)S(\theta)S(\phi) & C(\theta)S(\phi) \\ S(\psi)S(\phi) + C(\psi)S(\theta)C(\phi) & -C(\psi)S(\phi) + S(\psi)S(\theta)C(\phi) & C(\theta)C(\phi) \end{bmatrix} \quad (1)$$

, where ϕ, θ, and ψ are the Euler angles, and $C(.)$ and $S(.)$ are notations for $cos(.)$ and $sin(.)$ respectively. If a small angles for ϕ and θ are assumed, then the corresponding time derivatives of Euler angles are equal to the quadrotor angular velocity expressed in {B}. The DH table for the 2-Link manipulator are derived and presented in [12] from which one can find the transformation matrices, A_0^B, A_1^0, and A_2^1, between the frames.

2.1 Forward Kinematics

The position and orientation of the end-effector expressed in the inertial frame, $\{I\}$, are defined as $\eta_{e_1} = [x_e, y_e, z_e]^T$ and $\eta_{e_2} = [\phi_e, \theta_e, \psi_e]^T$, respectively. The transformation matrix from the body frame to the inertial frame is A_B^I and is given as:

$$A_B^I = R_B^I * transl(X, Y, Z) \tag{2}$$

where R_B^I is a rotation matrix expressed in $(4x4)$ homogeneous form , and $transl(X, Y, Z)$ is $(4x4)$ homogeneous transform matrix that describes the translation along X, Y and Z-axes of the inertial frame. The total transformation matrix that relates the end-effector frame to the inertial frame is T_2^I, which is given by:

$$T_2^I = A_B^I A_0^B A_1^0 A_2^1 \tag{3}$$

Define the general form for this transformation matrix as a function of end-effector variables (η_{e_1} and η_{e_2}), as following:

$$T_e = \begin{bmatrix} r_{11} & r_{12} & r_{13} & x_e \\ r_{21} & r_{22} & r_{23} & y_e \\ r_{31} & r_{32} & r_{33} & z_e \\ 0 & 0 & 0 & 1 \end{bmatrix} \tag{4}$$

By equating (3) and (4), expressions for the parameters of T_e (r_{ij}, x_e, y_e, and z_e; $i, j = 1, 2, 3$) can be found, from which the values of the end-effector variables can be determined. Euler angles of the end-effector (ϕ_e, θ_e and ψ_e) can be computed from the rotation matrix of T_e.

2.2 Inverse Kinematics

The inverse kinematics problem consists of determining the quadrotor/joint space variables (X, Y, Z, ψ, θ_1, and θ_2) as function of the operational coordinates (η_{e_1} and η_{e_2}).

We aim for point-to-point control since we target end-effector control during picking and placing operations (target positions are reset), so we put $\phi = \theta = 0$ in (3) and obtain the following:

$$T_2^I = \begin{bmatrix} C(\psi)S(\theta_2) + C(\theta_1)C(\theta_2)S(\psi) & C(\psi)C(\theta_2) - C(\theta_1)S(\psi)S(\theta_2) & S(\psi)S(\theta_1) & X + L_1C(\theta_1)S(\psi) + L_2C(\psi)S(\theta_2) + L_2C(\theta_1)C(\theta_2)S(\psi) \\ S(\psi)S(\theta_2) - C(\psi)C(\theta_1)C(\theta_2) & C(\theta_2)S(\psi) + C(\psi)C(\theta_1)S(\theta_2) & -C(\psi)S(\theta_1) & Y - L_1C(\psi)C(\theta_1) + L_2S(\psi)S(\theta_2) - L_2C(\psi)C(\theta_1)C(\theta_2) \\ -C(\theta_2)S(\theta_1) & S(\theta_1)S(\theta_2) & C(\theta_1) & Z - L_0 - L_1S(\theta_1) - L_2C(\theta_2)S(\theta_1) \\ 0 & 0 & 0 & 1 \end{bmatrix} \tag{5}$$

Then, from (4) and (5), the inverse kinematics of the system can be derived. The inverse orientation has three cases as following:

CASE 1: Suppose that not both of r_{13} and r_{23} are zero. Then from (5), we deduce that $sin(\theta_1) \neq 0$ and $r_{33} \neq \pm 1$. Then, $cos(\theta_1) = r_{33}$ and $sin(\theta_1) = \pm \sqrt{1 - r_{33}^2}$ and thus,

$$\theta_1 = atan2(\pm\sqrt{1 - r_{33}^2}, r_{33}) \tag{6}$$

and

$$\psi = atan2(\pm r_{13}, \mp r_{23}) \tag{7}$$

$$\theta_2 = atan2(\pm r_{32}, \mp r_{31}) \tag{8}$$

Thus, there are two solutions depending on the sign chosen for $sin(\theta_1)$. If $r_{13} = r_{23} = 0$, then the fact that T_e is orthogonal implies that $r_{33} = \pm 1$.

CASE 2: If $r_{13} = r_{23} = 0$ and $r_{33} = 1$, then $cos(\theta_1) = 1$ and $sin(\theta_1) = 0$, so that $\theta_1 = 0$. In this case, from the rotation matrix of (5), the sum $\theta_2 + \psi$ can be determined as:

$$\theta_2 + \psi = atan2(r_{11}, r_{12}) \tag{9}$$

We can assume any value for ψ and get θ_2. Therefore, there are infinite number of solutions.

CASE 3: If $r_{13} = r_{23} = 0$ and $r_{33} = $ -1, then $cos(\theta_1) = $ -1 and $sin(\theta_1) = 0$, so that $\theta_1 = \pi$. In this case, from (5), $\theta_2 - \psi$ can be determined as:

$$\theta_2 - \psi = atan2(r_{11}, r_{12}) \tag{10}$$

One can assume any value for ψ and get θ_2. Therefore, there are infinite number of solutions. In cases 2 and 3, one may put $\psi = 0$ and get θ_2. Finally, the inverse position is determined as following:

$$X = x_e - (L_1 C(\theta_1)S(\psi) + L_2 C(\psi)S(\theta_2) + L_2 C(\theta_1)C(\theta_2)S(\psi)) \tag{11}$$

$$Y = y_e - (-L_1 C(\psi)C(\theta_1) + L_2 S(\psi)S(\theta_2) - L_2 C(\psi)C(\theta_1)C(\theta_2)) \tag{12}$$

$$Z = z_e - (-L_0 - L_1 S(\theta_1) - L_2 C(\theta_2)S(\theta_1)) \tag{13}$$

3. Dynamic Analysis

The equations of motion of the proposed robot are derived in details in [12]. For the manipulator dynamics, Recursive Newton Euler method [15] is used to derive the equations of motion. Since the quadrotor is considered to be the base of the manipulator, the initial linear and angular velocities and accelerations,

used in Newton Euler algorithm, are that of the quadrotor expressed in body frame. Applying Newton Euler algorithm to the manipulator considering that the link (with length L_0) that is fixed to the quadrotor is the base link, manipulator's equations of motion can be obtained, in addition to, the forces and moments, from manipulator, that affect the quadrotor.

The dynamical model of the quadrotor-manipulator system can be written as follows:

$$M(q)\ddot{q} + C(q,\dot{q})\dot{q} + G(q) = \tau - d_{ex}, \tag{14}$$

where $q = [X, Y, Z, \phi, \theta, \psi, \theta_1, \theta_2]^T \in R^8$ is the vector of the generalized and redundant coordinates, and there are two second order nonholonomic constraints [12] which can reduce the 8 variables into 6 independent coordinates, $M \in R^{8x8}$ represents the symmetric and positive definite inertia matrix of the combined system, $C \in R^8$ is the matrix of Coriolis and centrifugal terms, $G \in R^8$ is the vector of gravity terms, $\tau \in R^8$ is the vector of the system applied forces and torques which are functions of the actuator's inputs ($F_1, F_2, F_3, F_4, \tau_{m_1}$, and τ_{m_2}), and $d_{ex} \in R^8$ is the vector that represents the external disturbances.

We proposed a methodology for the identification process of the proposed system and implemented it as described in details in [16]. The identified parameters are given in [17].

4. Controller Design

The desired values for the end-effector's position (x_{e_d}, y_{e_d} and z_{e_d}) and orientation (ϕ_{e_d}, θ_{e_d} and ψ_{e_d}) are converted to the desired values of the quadrotor (X_d, Y_d, Z_d and ψ_d) and joints variables (θ_{1_d} and θ_{2_d}) through the inverse kinematics that are derived in section 2. Next, these values are applied to a trajectory generation algorithm which will provide Quintic polynomial trajectories [14] as the reference trajectories for quadrotor/joint space. By using these types of trajectories for the joint space control, we can avoid the undesirable system jerks. The control design criteria are to achieve system stability and zero position error in the quadrotor/joint space and consequently for the end-effector's desired position and orientation (η_{e_1} and η_{e_2}), under the effect of picking and placing a payload, changing the operating region of the system, and measurement noise.

4.1 Disturbance Observer-based Control

Disturbance Observer (DOb)-based controller is one of the most popular methods in the field of robust motion control due to its simplicity and computational efficiency. The authors in [18, 19] present the principles of DOb-based control system. In DOb based robust motion control systems, internal and external disturbances are observed by DOb, and the robustness is simply achieved by feeding-back the estimated disturbances in an inner-loop. Another controller is designed in an outer loop so that the performance goals are achieved without considering internal and external disturbances. In [20–23], DOb-

based control technique has been applied to robotic systems and showed efficient performance. In [24], a Robust Internal-loop Compensator (RIC), which is a DOb based controller, is designed to achieve the trajectory tracking in the quadrotor/joint space and provides satisfactory performance.

A block diagram of the DOb controller for the system described in (14) is shown in Fig. 3. Since the vehicle (quadrotor) is an under-actuated system, i.e., only 4 independent control inputs are available against the 6 DOF, the position and the yaw angle are usually the controlled variables, while pitch and roll angles are used as intermediate control inputs for position control. Hence, the vector q can be rewritten by defining the generalized coordinates $\zeta = [X, Y, Z, \psi, \theta_1, \theta_2]^T$ and the redundant coordinates $\sigma = [\theta, \phi]^T$. Therefore, two controllers are designed; the first one is the ζ controller which will be used to generate the reference values for the roll and pitch angles that are fed to the second one which is σ controller. However, the response of the σ controller must be much faster than that of the quadrotor position controller such that it can track the changes in the position controller. In this figure, $M_n \in R^{8x8}$ is the system nominal inertia matrix, τ and τ^{des} are the robot and desired inputs, respectively, $P = Diag([g_1, ..., g_i, ..., g_8])$ with g_i is the bandwidth of the ith variable of q, $Q(s) = Diag([\frac{g_1}{s+g_1}, ..., \frac{g_i}{s+g_i}, ..., \frac{g_8}{s+g_8}]) \in R^{8x8}$ is the matrix of the low pass filter of DOb, and τ^{dis} represents the system disturbances. Let us assume that the velocity is estimated by using a low pass filter, $Q_v(s) = Diag([\frac{g_{v_1}}{s+g_{v_1}}, ..., \frac{g_{v_i}}{s+g_{v_i}}, ..., \frac{g_{v_8}}{s+g_{v_8}}]) \in R^{8x8}$, with cut-off frequency of $P_v = Diag([g_{v_1}, ..., g_{v_i}, ..., g_{v_8}])$. Each of these variables is separated for ζ and σ such that M_{n_ζ}, P_ζ, Q_ζ, and τ_ζ for ζ controller and similarly for the σ controller. The system disturbance τ^{dis} can be assumed as:

$$\tau^{dis} = (M_n - M(q))\ddot{q} + \tau^s; \qquad \tau^s = C(q, \dot{q})\dot{q} + G(q) + d_{ex} \tag{15}$$

The estimated disturbance $\widehat{\tau}^{dis}$ can be formulated from Fig. 3 as:

$$\widehat{\tau}^{dis} = \widehat{P}(s)(\tau^{des} - M_n\ddot{q}); \qquad \widehat{P}(s) = Diag([\frac{g_1}{s}, .., \frac{g_i}{s}, .., \frac{g_8}{s}]) \tag{16}$$

After the disturbances are estimated and canceled by the inner-loop of DOb, the outer-loop external controller can be used to achieve the desired performance of the system which becomes a double integrator system. Concerning the outer-loop, define; K_P and $K_D \in R^{8x8}$ be the proportional and derivative gains of PD controllers, receptively, $\ddot{q}^{des}$ is the desired acceleration, and q^{ref}, $\dot{q}^{ref}$, and $\ddot{q}^{ref}$ are the references for angle, velocity, and acceleration, respectively. The desired values σ^{ref} for the intermediate controller are obtained from the output of position controller, τ_ζ, through the following relation:

$$\sigma^{ref} = \frac{1}{\tau_\zeta(3)} \begin{bmatrix} C(\psi) & S(\psi) \\ S(\psi) & -C(\psi) \end{bmatrix} \begin{bmatrix} \tau_\zeta(1) \\ \tau_\zeta(2) \end{bmatrix} \tag{17}$$
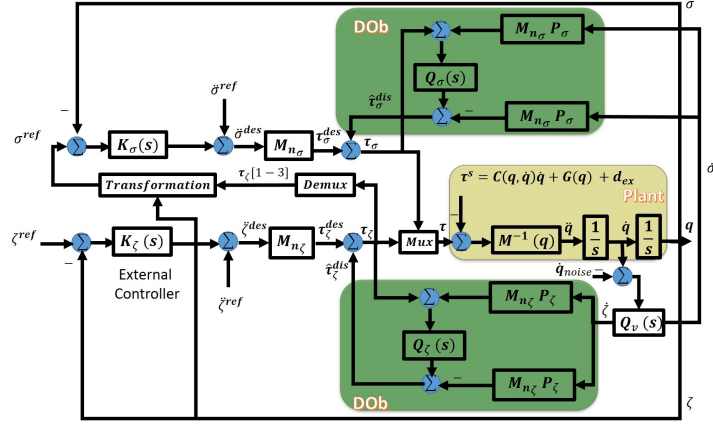
7

Figure 3: Block diagram of DOb-base controller

4.2 Stability Analysis

To simplify the analysis, let us have the following assumptions; The system equation of motion both σ and ζ are combined such that they form an equation of motion of robotic system, the system is not influenced by external disturbances, $d_{ex} = 0$, as well as measurement noise and the velocity filter $Q_v(s)$, and the bandwidths of DObs are the same; $g_1 = g_2 = ... = g_8 = g_c$. By applying the DOb-based robust motion control algorithm, the dynamic model of the whole system will be:

$$M(q)\ddot{q} + C(q, \dot{q})\dot{q} + G(q) = \tau^{des} + \widehat{\tau}^{dis} \tag{18}$$

The desired torque, as in Fig. 3, is

$$\tau^{des} = M_n \ddot{q}^{des}, \tag{19}$$

where

$$\ddot{q}^{des} = \ddot{q}^{ref} + K_P e + K_D \dot{e}; \qquad e = q^{ref} - q \tag{20}$$

From (16 and 19) the estimated disturbance is:

$$\widehat{\tau}^{dis} = g_c M_n (\dot{q}^{des} - q) \tag{21}$$

Substituting from (19 and 21) into (18) will give:

$$M(q)\ddot{q} + C(q, \dot{q})\dot{q} + G(q) = M_n \ddot{q}^{des} + g_c M_n (\dot{q}^{des} - q) \tag{22}$$

The error dynamics for $e_D = \dot{q}^{des} - \dot{q}$ is:

$$M(q)\dot{e}_D + C(q, \dot{q})e_D + g_c M_n e_D = \delta \tag{23}$$

8

where

$$\delta = \Delta M(q)\ddot{q}^{des} + C(q,\dot{q})\dot{q}^{des} + G(q); \qquad \Delta M(q) = M(q) - M_n, \tag{24}$$

Equation (23) represents the error dynamics of DOb-based robust control of the quadrotor manipulation system. Assuming the following Lyapunov function:

$$V = \frac{1}{2}e_D^T M(q) e_D \tag{25}$$

The time derivative of this function is:

$$\dot{V} = e_D^T M(q)\dot{e}_D + \frac{1}{2}e_D^T \dot{M}(q) e_D \tag{26}$$

Substituting from (23),

$$\dot{V} = e_D^T \delta - g e_D^T M_n e_D + \frac{1}{2}e_D^T (\dot{M}(q) - 2C(q,\dot{q})) e_D \tag{27}$$

The dynamic equation of motion (14) posses several well known properties [25, 26]. These properties will be used to complete the stability analysis and they are stated as follows:

$$\lambda_M^{min} I \leq M(q) \leq \lambda_M^{max} I$$

$$\|C(q,\dot{q})\dot{q}^*\| \leq \lambda_C \|\dot{q}\| \|\dot{q}^*\|$$

$$\|G(q)\| \leq \lambda_G$$

$$\nu^T (\dot{M}(q) - 2C(q,\dot{q}))\nu = 0 \tag{28}$$

where $\dot{M}(q) - 2C(q,\dot{q})$ is a skew-symmetric matrix, $\nu \in R^8$ represents a 8-dimensional vector, and λ_M^{min}, λ_M^{max}, λ_C, and λ_G are positive real constants. Substituting from (28) into (27):

$$\dot{V} = e_D^T \delta - g e_D^T M_n e_D \tag{29}$$

Substituting from (24) in (29):

$$\dot{V} = -g_c e_D^T M_n e_D - e_D^T \Delta M(q)\ddot{q}^{des} - e_D^T (C(q,\dot{q})\dot{q}^{des} + G(q)) \tag{30}$$

Form (28), a sufficient condition of the stability is:

$$\dot{V} \leq g_c \lambda_{M_n}^{min} \|e_D\|_2^2 + \lambda_{\Delta M}^{max} \|\ddot{q}^{des}\|_2 \|e_D\|_2 + \lambda_C \|\dot{q}\|_2 \|\dot{q}^{des}\|_2 \|e_D\|_2 + \lambda_G \|e_D\|_2 \leq 0 \tag{31}$$

9

Equation (31) shows that the time derivative of the Lyapunov function, $\dot{V}$, is negative outside of the compact set $\Upsilon_\Gamma \{\|e_D\|_2 > \Gamma\}$ where Γ is defined as follows:

$$\Gamma = \frac{\lambda_{\Delta M}^{max}\left\|\ddot{q}^{des}\right\|_2 + \lambda_C \|\dot{q}\|_2 \left\|\dot{q}^{des}\right\|_2 + \lambda_G}{g_c \lambda_{M_n}^{min}} \tag{32}$$

Therefore, all solutions that start outside of Υ_Γ enter this set within a finite time, and remain inside the set for future time. As a result, the error dynamics, e_D, is uniformly ultimately bounded with respect to Υ_Γ.

Equation (26) and (27) show that as the bandwidth of DOb and / or nominal inertia matrix are increased (i.e. $M_n \geq M(q)$), the Lyapunov function decreases faster and the stability of the position control system is improved. Therefore, we choose the M_{n_σ} to M_σ ratio to be much higher than that between M_{n_ζ} and M_ζ such that the response speed of σ is much higher than that of ζ.

From the above derivations, we found that increasing the nominal inertia matrix M_n than the actual one $M(q)$ as well as DOb bandwidth, g_i, will improve the system stability. However, there are constraints on these values which are investigated in [27]. By assuming that the DOb will estimate and reject the disturbances accurately, the following constraints on the DOb parameters can be derived:

$$\rho P \leq \frac{P_v}{2}, \qquad \rho = \frac{M_n}{M}$$
$$\frac{1}{\rho} < 1 + P\frac{K_D}{K_P} + \frac{K_D}{P} + \frac{K_D^2}{K_P} \tag{33}$$

Equation (33) sets the constraints on the outer loop parameters and the robustness condition.

5. Simulation Results

The model of the considered robot and the control laws for both FMRLC and DOb techniques are simulated in MATLAB. In order to simulate the measured data, the following assumption have been made: a normally distributed measurement noise, with mean of 10^{-3} and standard deviation of 5×10^{-3}, has been added to the measured signals.

Parameters of DOb-based control is given in Table 1. The design details and parameters of FMRLC can be found in [17]. The two controllers are tested to stabilize and track the desired quadrotor/joint space trajectories under the effect of picking a payload of value $150g$ at instant $15s$ and placing it at instant $55s$.

The simulation results of both FMRLC and DOb based controllers in quadrotor/joint space are presented in Fig. 4. Fig. 5 shows response of system in the task space (the actual end-effector position and orientation can be found from the forward kinematics). These results show that both DOb and FMRLC are able to track the desired trajectories, with different operating regions, and with picking, holding, and

Table 1: Parameters for DOb-based control

Par.	Value	Par.	Value
M_{n_ζ}	$Diag\{2, 2, 2, 0.5, 0.5, 0.5\}$	M_{n_σ}	$Diag\{0.5, 0.5\}$
K_{P_ζ}	$Diag\{10, 10, 20, 10, 10, 10\}$	K_{P_σ}	$Diag\{7, 7\}$
K_{D_ζ}	$Diag\{7, 7, 15, 10, 10, 10\}$	K_{D_σ}	$Diag\{3, 3\}$
g_i	1	g_{v_i}	100

placing a payload. Figs. 6 shows the control effort, the required thrust forces and manipulator torques, in case of DOb and FMRLC respectively.

These results indicate that the FMRLC suffers from chattering problem which may either damage the actuator or can not be achieved experimentally. Moreover, since the DOb is simpler than FMRLC, the computation time for control laws of DOb is very small compared to that of FMRLC. In the simulation model, the computation time of DOb is lower than that of FMRLC by 55%. Therefore, DOb is recommended to be implemented in experimental work.
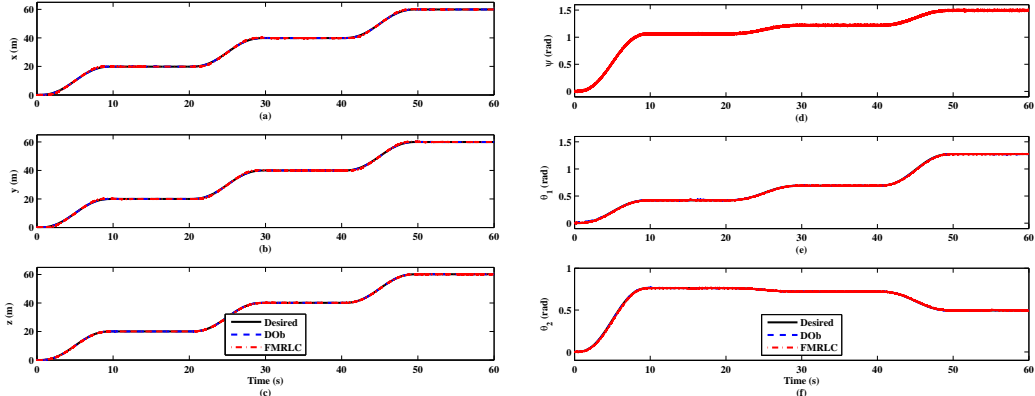

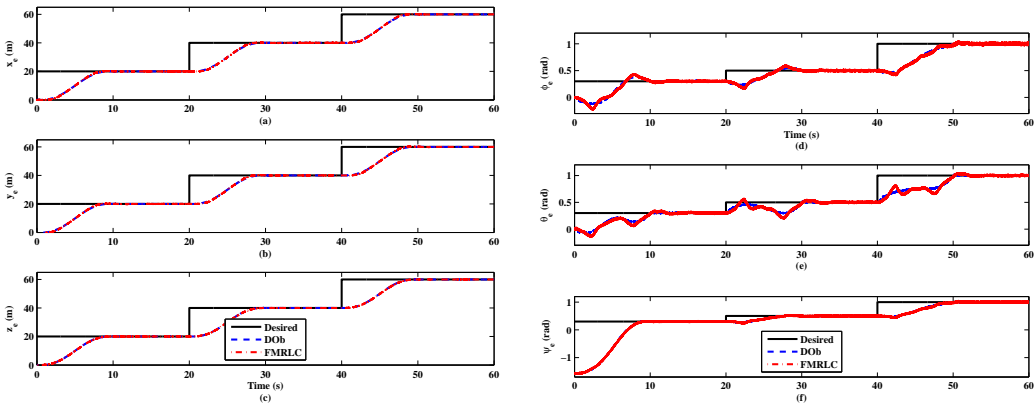Figure 4: The actual response in the quadrotor/joint space

Figure 5: The actual response in the end-effector space

6. Conclusion

A new aerial manipulation robot called "Quadrotor Manipulation System" is briefly described. This proposed robot finds solutions for the limitations of the current aerial manipulation system. Kinematic and dynamic analysis of the proposed system are carried out. A closed forms for system forward/inverse
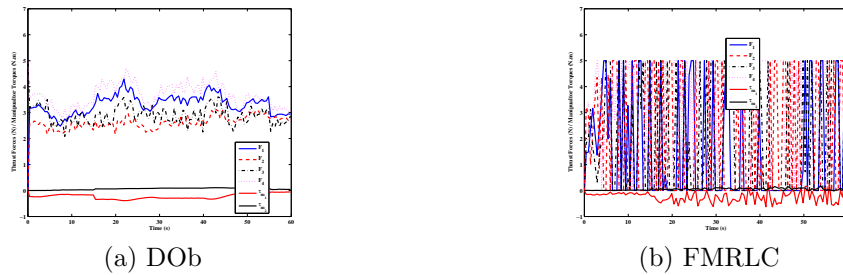
| (a) DOb | (b) FMRLC |

Figure 6: The required controller efforts

kinematics, are derived. However, the form for inverse kinematics is suitable for using in point-to-point control in the task space. This is sufficient because we target end-effector control during picking and placing operations. DOb-based control design is presented to control the proposed system. The stability analysis is proved for this controller. The DOb-based controller is compared with previously developed FMRLC controller. These controllers are tested to achieve trajectory tracking under the effect of picking/placing a payload, changing the operating region, and the measurement noise. The system is simulated using MATLAB/SIMULINK. Simulation results indicate the feasibility of the proposed system and the effectiveness of the proposed kinematic analysis. In addition, the DOb technique has low computation time. Unlike DOb, FMRLC provide chattering in the required control efforts. Therefore, the DOb is highly recommended for implementation in real time to test experimentally the proposed system which will be carried out in a future work.

Acknowledgment

References

[1] S. Gupte, P. I. T. Mohandas, and J. M. Conrad, "A survey of quadrotor unmanned aerial vehicles," in *Southeastcon, 2012 Proceedings of IEEE*, pp. 1–6, IEEE, 2012.

[2] D. Mellinger, Q. Lindsey, M. Shomin, and V. Kumar, "Design, modeling, estimation and control for aerial grasping and manipulation," in *2011 IEEE/RSJ International Conference on Intelligent Robots and Systems (IROS)*, pp. 2668–2673, IEEE, 2011.

[3] M. Bisgaard, A. la Cour-Harbo, and J. Dimon Bendtsen, "Adaptive control system for autonomous helicopter slung load operations," *Control Engineering Practice*, vol. 18, no. 7, pp. 800–811, 2010.

[4] N. Michael, J. Fink, and V. Kumar, "Cooperative manipulation and transportation with aerial robots," *Autonomous Robots*, vol. 30, no. 1, pp. 73–86, 2011.

[5] A. Torre, D. Mengoli, R. Naldi, F. Forte, A. Macchelli, and L. Marconi, "A prototype of aerial manipulator," in *Intelligent Robots and Systems (IROS), 2012 IEEE/RSJ International Conference on*, pp. 2653–2654, IEEE, 2012.

[6] F. Huber, K. Kondak, K. Krieger, D. Sommer, M. Schwarzbach, M. Laiacker, I. Kossyk, S. Parusel, S. Haddadin, and A. Albu-Schaffer, "First analysis and experiments in aerial manipulation using fully actuated redundant robot arm," in *Intelligent Robots and Systems (IROS), 2013 IEEE/RSJ International Conference on*, pp. 3452–3457, IEEE, 2013.

[7] C. M. Korpela, T. W. Danko, and P. Y. Oh, "Mm-uav: Mobile manipulating unmanned aerial vehicle," *Journal of Intelligent & Robotic Systems*, vol. 65, no. 1-4, pp. 93–101, 2012.

[8] A. Jimenez-Cano, J. Martin, G. Heredia, A. Ollero, and R. Cano, "Control of an aerial robot with multi-link arm for assembly tasks," in *Robotics and Automation (ICRA), 2013 IEEE International Conference on*, pp. 4916–4921, IEEE, 2013.

[9] G. Heredia, A. Jimenez-Cano, I. Sanchez, D. Llorente, V. Vega, J. Braga, J. Acosta, and A. Ollero, "Control of a multirotor outdoor aerial manipulator," in *Intelligent Robots and Systems (IROS 2014), 2014 IEEE/RSJ International Conference on*, pp. 3417–3422, IEEE, 2014.

[10] R. Cano, C. Pérez, F. Pruaño, A. Ollero, and G. Heredia, "Mechanical design of a 6-dof aerial manipulator for assembling bar structures using uavs," *RED-UAS*, 2013.

[11] F. Caccavale, P. Chiacchio, A. Marino, and L. Villani, "Six-dof impedance control of dual-arm cooperative manipulators," *Mechatronics, IEEE/ASME Transactions on*, vol. 13, no. 5, pp. 576–586, 2008.

[12] A. Khalifa, M. Fanni, A. Ramadan, and A. Abo-Ismail, "Modeling and control of a new quadrotor manipulation system," in *2012 IEEE/RAS International Conference on Innovative Engineering Systems*, pp. 109–114, IEEE, 2012.

[13] S. Kim, S. Choi, and H. J. Kim, "Aerial manipulation using a quadrotor with a two dof robotic arm," in *Intelligent Robots and Systems (IROS), 2013 IEEE/RSJ International Conference on*, pp. 4990–4995, IEEE, 2013.

[14] J. Leishman, *Principles of Helicopter Aerodynamics*. Cambridge University Press, 2000.

[15] L.-W. Tsai, *Robot analysis: the mechanics of serial and parallel manipulators*. Wiley-Interscience, 1999.

[16] M. Elsamanty, A. Khalifa, M. Fanni, A. Ramadan, and A. Abo-Ismail, "Methodology for identifying quadrotor parameters, attitude estimation and control," in *Advanced Intelligent Mechatronics (AIM), 2013 IEEE/ASME International Conference on*, pp. 1343–1348, IEEE, 2013.

[17] A. Khalifa, M. Fanni, A. Ramadan, and A. Abo-Ismail, "Adaptive intelligent controller design for a new quadrotor manipulation system," in *Systems, Man, and Cybernetics (SMC), 2013 IEEE International Conference on*, pp. 1666–1671, IEEE, 2013.

[18] B. K. Kim and W. K. Chung, "Performance tuning of robust motion controllers for high-accuracy positioning systems," *Mechatronics, IEEE/ASME Transactions on*, vol. 7, no. 4, pp. 500–514, 2002.

[19] S. Li, J. Yang, W.-h. Chen, and X. Chen, *Disturbance observer-based control: methods and applications*. CRC Press, 2014.

[20] E. Sariyildiz, H. Yu, K. Yu, and K. Ohnishi, "A nonlinear stability analysis for the robust position control problem of robot manipulators via disturbance observer," in *Mechatronics (ICM), 2015 IEEE International Conference on*, pp. 28–33, IEEE, 2015.

[21] H.-T. Choi, S. Kim, J. Choi, Y. Lee, T.-J. Kim, and J.-W. Lee, "A simplified model based disturbance rejection control for highly accurate positioning of an underwater robot," in *Oceans-St. John's, 2014*, pp. 1–5, IEEE, 2014.

[22] X.-y. Wang and Y.-j. Pi, "Trajectory tracking control of a hydraulic parallel robot manipulator with lumped disturbance observer," *International Journal of Robotics and Automation*, vol. 28, no. 2, 2013.

[23] M. Chen, B. Jiang, and R.-X. Cui, "Robust control for rigid robotic manipulators using nonlinear disturbance observer," *International Journal of Robotics and Automation*, vol. 29, no. 3, 2014.

[24] A. Khalifa, M. Fanni, A. Ramadan, and A. Abo-Ismail, "Controller design of a new quadrotor manipulation system based on robust internal-loop compensator," in *Autonomous Robot Systems and Competitions (ICARSC), 2015 IEEE International Conference on*, pp. 97–102, IEEE, 2015.

[25] P. J. From, J. T. Gravdahl, and K. Y. Pettersen, *Vehicle-Manipulator Systems*. Springer, 2014.

[26] M. W. Spong, S. Hutchinson, and M. Vidyasagar, *Robot modeling and control*, vol. 3. Wiley New York, 2006.

[27] E. Sariyildiz and K. Ohnishi, "Stability and robustness of disturbance-observer-based motion control systems," *Industrial Electronics, IEEE Transactions on*, vol. 62, no. 1, pp. 414–422, 2015.

Biographies

Ahmed Khalifa. received the B.S. degree in Industrial Electronics and Control Engineering from Monofiya University, Egypt, in 2009, and the M.Sc. degree in Mechatronics and Robotics Engineering from Egypt-Japan University of Science and Technology (E-JUST), Alexandria, Egypt, in 2013. He is currently pursuing the Ph.D. degree in Mechatronics and Robotics Engineering at E-JUST.

Mohamed Fanni. received the B.E. and M.Sc. degrees in mechanical engineering from Faculty of Engineering of both Cairo University and Mansoura University, Egypt, in 1981 and 1986, respectively and the Ph.D. degree in engineering from Karlsruhe University, Germany, 1993. He is an Associate Professor with Innovation, Graduate School of Engineering Science, Egypt-Japan University of Science and Technology E-JUST, Alexandria, on leave from Production Engineering & Mechanical Design Department, Faculty of Engineering, Mansoura University, Egypt. His major research interests include robotics engineering, automatic control, and Mechanical Design. His current research focuses on Design & Control of Mechatronic Systems, Surgical Manipulators, Teleoperation systems and Flying/Walking Robots.